Metal Nanoplasmas as Bright Sources of Hard X-Ray Pulses

P. P. Rajeev, P. Taneja, P. Ayyub, A. S. Sandhu, and G. Ravindra Kumar*
Tata Institute of Fundamental Research, 1, Homi Bhabha Road, Mumbai 400 005, India
(Received 11 April 2002; published 18 March 2003)

We report significant enhancements in light coupling to intense-laser-created solid plasmas via surface plasmon and "lightning rod" effects. We demonstrate this in metal nanoparticle-coated solid targets irradiated with 100 fs, 806 nm laser pulses, focused to intensities $\sim 10^{14}$–10^{15} W cm^{-2}. Our experiments show a 13-fold enhancement in hard x-ray yield (10–200 keV) emitted by copper nanoparticle plasmas formed at the focal volume. A simple model explains the observed enhancement quantitatively and provides pointers to the design of structured surfaces for maximizing such emissions.

DOI: 10.1103/PhysRevLett.90.115002 PACS numbers: 52.25.Os, 42.65.Re, 52.38.–r, 52.50.Jm

The interaction of intense, ultrashort laser pulses with solid plasmas is a very important research area in basic physics. It offers a unique opportunity for understanding the explosive ionization of matter, for studies of physical systems which possess high energy coupled with high density, and for simulation of intrastellar conditions. Such plasmas also offer great promise as micron-sized sources of ultrashort x rays, in areas such as lithography and time resolved diffraction [1,2]. Methods to enhance the x-ray yield are of great importance, and the influence of various laser and target conditions is widely investigated. Preformed plasmas [3,4] yield significant enhancements at the cost of an increase in the x-ray pulse duration. Recent literature reports impressive enhancements in soft [5] and moderately hard x-ray regions [6] using structured surfaces, viz., gratings [5,7,8], "velvet" coatings [9], and porous and nanocylinder [4,8,10] targets. However, little attention has been paid to examining ways of improving the very hard (>10 keV) x-ray yield, a signature of hot electrons created in the plasma [11]. Enhanced x-ray yield, therefore, implies enhanced hot electron production, an issue that is of immense interest in inertial fusion research [12] and particle acceleration [13]. In this Letter, we demonstrate a method to enhance hard x-ray bremsstrahlung by coating nanoparticles (NP) on optically smooth metal targets. We report a 13-fold enhancement in the total emission in the 10–200 keV range using copper NP-coated targets and show that they yield hotter electrons in comparison to optically polished, uncoated targets. These results are well explained by a simple model that invokes local electric field enhancement. In addition, our model provides clear guidelines to the design of surface microstructures that would maximize hot electron and x-ray yields. The giant enhancement in nonlinearity that such fractal structures provide [14] and the ease of patterning of such targets can prove invaluable in the design of efficient ultrashort x-ray sources.

Our Ti:Sapphire laser system generates 806 nm, 100 fs, 5 mJ pulses with a contrast ratio of 10^5 on picosecond time scales. p-polarized laser pulses are focused on targets housed in a vacuum chamber at 10^{-3} Torr [15]. A 1 mJ pulse yields a peak intensity of 1.3×10^{15} W cm^{-2} at a typical focal spot size of 40 μm. The target is constantly moved in order to avoid multiple laser hits at the same spot. X-ray emission from the plasma is observed in the plane of incidence, at 45° to the target normal, with a NaI (Tl) scintillation detector, wherein energy of the incident photon determines the amplitude of the detector output, giving energy-dispersed yields in the observed energy range. The detector efficiency is $\sim$100% in the range 10–500 keV [16] and has 6.1% energy resolution at 661.6 keV. The detector is gated with the laser pulse and the signal is collected only in a time window of 30 μs, to ensure background-free acquisition [15]. The observed spectrum is essentially bremsstrahlung as the characteristic emissions are blocked by a 3-mm BK-7 window.

We use two types of Cu NP-coated targets, one with spherical (inset in Fig. 1) and the other with ellipsoidal nanoparticles (SNP and ENP, respectively). Their emission is compared with highly polished copper targets. Cu nanoparticles are deposited by high pressure dc sputtering [17] on polished copper disks (held at 0 °C for spherical particles and at -50 °C for ellipsoids of aspect ratio 1.5). The resulting nanocrystalline films are optically flat and 1 μm thick. The crystallographic domain size (d_{XRD}) is obtained from x-ray diffraction line broadening, using the Scherrer technique. For a film deposited in 180 mTorr Ar environment at a sputtering power of 200 W, we obtain $d_{\mathrm{XRD}} = 15$ nm. The aspect ratio is obtained from a comparison of d_{XRD} calculated from (111) and (200) diffraction lines. The essentially specular reflection spectra are measured (Fig. 1) using a Shimadzu UV-2100 spectrophotometer.

The reflectivity data were fitted to the Drude model for $\lambda > 650$ nm, below which the interband transitions contribute to the dielectric function. Assuming a constant plasma frequency and with a collision frequency adjusted for a best fit, we get the effective permittivity ($\epsilon' + i\epsilon''$) of the NP-void composite as a function of λ. Using the generalized Bruggeman effective medium approximation

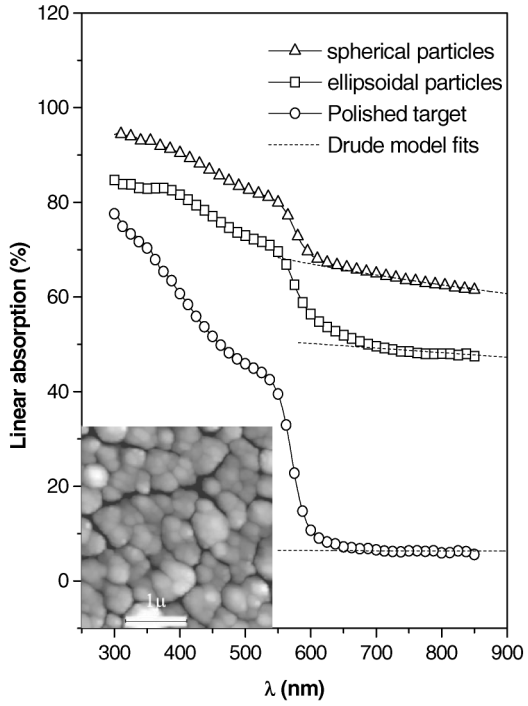

FIG. 1. Linear absorption spectra of polished and nanoparticle coated targets. Inset: scanning electron micrograph of SNP-coated target. The solid lines show Drude model fits.

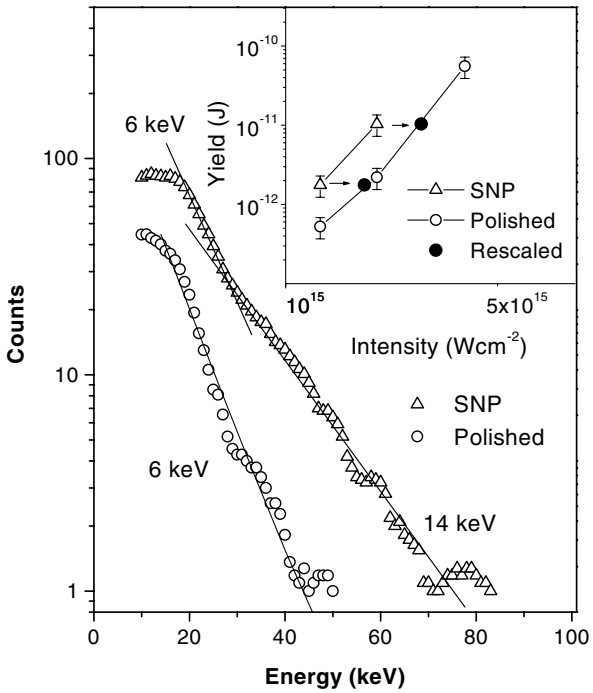

FIG. 2. Bremsstrahlung emission at 10°. Inset: variation of integrated emission with input laser intensity.

[18], the permittivities of the SNP and ENP are obtained as $-27 + i33$ and $-27 + i44.4$, respectively, as opposed to their bulk value $-27 + i2.5$. Extensive studies have been carried out on the variation of the dielectric constant with particle size [19,20]. The real part of the dielectric constant is shown to be unaffected in most systems, unless the particle size is extremely small. The imaginary part increases due to the limited electron mean-free path in the NP. The imaginary parts obtained above are, however, much larger than the theoretically predicted values [21] and this mismatch is possibly due to the factors such as particle size distribution and dipole interactions between particles that are excluded in these calculations. However, this discrepancy does not hamper the interpretations of our results, as the model does not critically depend on ϵ under our conditions.

To elucidate the role of nanoparticles in hot electron generation, we present data at two angles of incidence, 10° and 45°. Figure 2 shows a comparison of bremsstrahlung emission at 10°, measured at a solid angle of 720 μsr, from the polished and SNP-coated targets irradiated at 2.0×10^{15} W cm^{-2}. The total energy emitted per pulse in the above range from the polished target is 2.2×10^{-12} J, whereas it is 1×10^{-11} J from the NP-coated target, assuming isotropic emission. It is clearly evident that there are two temperature components (6 and 14 keV) in the spectrum from the NP-coated target, while the higher component is at least 100 times weaker in the emission from the polished target. The excess absorption caused by local field enhancements could result in the higher temperature component as we show below.

Modification of electric field due to surface protrusions has been well studied in connection with second harmonic generation [22] and surface enhanced Raman scattering [23]. At higher intensities, the field resonance is known to be a major source of hot electrons in a cluster plasma [24]. However, this idea has not been utilized so far to understand the excess absorption of intense laser light on modulated surfaces.

For simplicity, the NP target is modeled as a collection of hemispheroids of permittivity ϵ, as shown in the inset in Fig. 3(a). Consider a p-polarized wave front of amplitude E, incident at an angle θ to the major axis of the spheroid. The model becomes much simpler with the assumption that the field along the major axis alone contributes to the enhancement. Thus, the resultant electric field at any point on the surface of the hemispheroid becomes $\mathbf{E}_r = \mathbf{E}_L^{\text{surf}} + E\cos\theta\hat{\boldsymbol{x}}$, where $\mathbf{E}_L^{\text{surf}}$ is the locally enhanced field and $E\cos\theta$ is the tangential component of the incident electric field on the metal surface. The enhanced local field on the surface of the spheroid is [22]

$$\mathbf{E}_L^{\text{surf}} = [L_{\parallel}^{\text{surf}} \sin\alpha\hat{\boldsymbol{\eta}} + L_{\perp}^{\text{surf}} \cos\alpha\hat{\boldsymbol{\xi}}]E\sin\theta, \qquad (1)$$

where $L_{\parallel}^{\text{surf}}$ and $L_{\perp}^{\text{surf}}$ are the local field correction factors given by

$$L_{\perp}^{\text{surf}} = L_R\epsilon/\left\{\epsilon - 1 + L_R\left[1 + i\frac{4\pi^2 V}{3\lambda^3}(1-\epsilon)\right]\right\} \qquad (2)$$

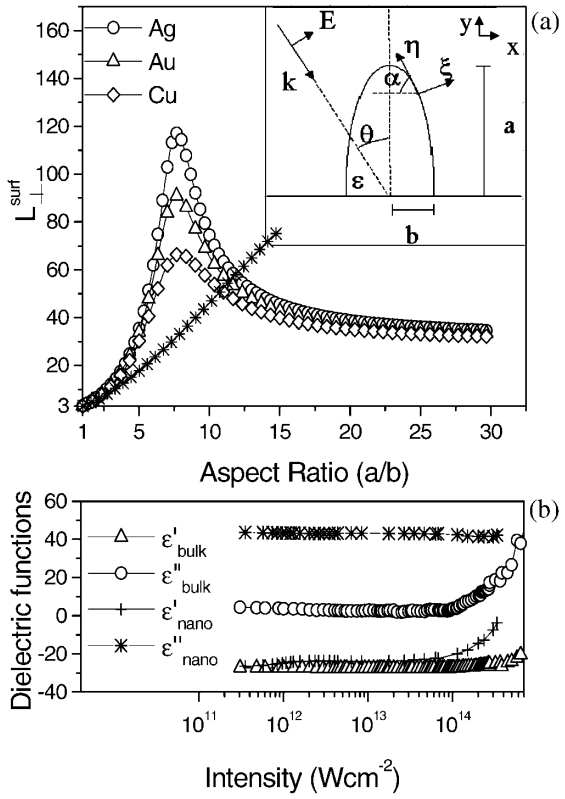

FIG. 3. (a) Enhancement factor at $\lambda = 806$ nm as a function of a/b for different metals, for $b = 7$ nm. $L_\perp^{\text{surf}}$ for $\epsilon = 10 + i30$ (plasma ϵ) is shown as stars. Inset: spheroidal model for nanoparticle. (b) Variation of dielectric functions of bulk Cu and ENP with intensity.

and $L_\parallel^{\text{surf}} = L_\perp^{\text{surf}}/\epsilon$, which is absent for metals. L_R is the lightning rod factor defined as $L_R = 1 - \xi Q'(\xi)/Q(\xi)$, where $\xi = [1 - (b/a)^2]^{-1/2}$ and $Q(\xi) = (\xi/2)\ln[(\xi + 1)/(\xi - 1)] - 1$. V is the volume of the spheroid. The maximum enhancement occurs towards the tip of the structure (low α values). The *effective intensity* at the tip ($\alpha = 0°$) is

$$I_r = I_{\text{in}}[(L_\perp^{\text{surf}})^2 \sin^2\theta + \cos^2\theta]. \quad (3)$$

The local field correction factors have a resonant behavior with a/b, the aspect ratio of the spheroid, as shown in Fig. 3(a). The dielectric constant ϵ is assumed to be a function of the particle diameter, viz. $\epsilon_{\text{nano}} = \epsilon'_{\text{bulk}} + i\epsilon''_{\text{bulk}}(1 + l/b)$, where l is the mean-free path of the electrons [19]. As is evident, silver NPs with aspect ratios close to the resonance values will yield greater enhancement than similar ones of gold and copper, although the absolute values could be affected by the possible plasma screening effects for large aspect ratios. Figure 3(b) provides the variation of dielectric functions of bulk Cu and ENP with input laser intensity, derived from self-reflectivity measurements similar to those in [25]. The deviation from room temperature values occurs only above 10^{14} W cm^{-2}. In Fig. 3(a), the resonance behavior depends on ϵ, although $L_\perp^{\text{surf}}$ does not depend critically on ϵ for small a/b values. Thus, in the present study, the room temperature values of ϵ will be quite good approximations in the calculations as $L_\perp^{\text{surf}}$ will be almost the same even for a drastically different plasma ϵ and the plasma shape remains intact as it is a femtosecond interaction.

Substituting the value of $L_\perp^{\text{surf}}$ for the spherical particle, we obtain $I_r/I_{\text{in}} \sim 1.4$, at $\theta = 10°$. Thus, *the NP-coated target is equivalent to a polished target with a rescaled (enhanced) intensity.* Figure 2 (inset) provides a comparison of the original data of yields from SNP and polished targets with the data obtained by rescaling the points for the NP target by $I_r = 1.4I$, and they are in good agreement.

Figure 4 presents a comparison of bremsstrahlung emission, measured at a solid angle of 22 msr, from the polished, SNP, and ENP-coated Cu targets irradiated at 45°, at 6.0×10^{14} W cm^{-2}. The total energy emitted per pulse from a polished target is 4.2×10^{-14} J, while it is 5.7×10^{-13} J using the ENP target, assuming isotropic emission. This amounts to a 13-fold enhancement in hot electron production. The spherical nanoparticles yield 1.4×10^{-13} J, giving approximately threefold enhancement as at 10°. Two temperature components, 3 and 11 keV, are observed in the spectrum from both NP-coated targets, whereas the higher component is hardly present in the emission from polished target. That the ellipsoidal nanoparticles give more than 4 times yield than the spherical particles is easily understood from Fig. 3 to be due to the enhancement of both lightning rod effect and plasmon resonance. An intensity rescaling, as above, gives $I_r/I_{\text{in}} \sim 9$. The higher component T_{hot} obtained using the ENP target corresponds to that obtained using a polished target at 9×10^{15} W cm^{-2} (close to the rescaled intensity for the ellipsoidal particle), as reported in our earlier work [26]. Since our model involves only an intensity rescaling, it does not assume any particular absorption mechanism, and all absorption scalings are equally applicable for NP targets as their dimensions are much smaller than λ.

The field enhancements are also responsible for enhanced nonlinearities [14]. Thus, multiphoton ionization in an NP target will be significantly enhanced, which in turn results in denser plasma formation and excess energy absorption. Because of the enhanced local fields and finite size of the surface protrusions, the oscillation energy of electrons reach a high value even at moderate intensities [27], yielding bremsstrahlung and characteristic emissions in hard x-ray regime, when they undergo collisions.

Intensity enhancements by the surface structures could form preplasma for low contrast pulses, which in turn give yield enhancements. In our case, however, preplasma formation is negligible as the threshold intensity for plasma formation is 10^{12}–10^{13} W cm^{-2} [28], quite above our prepulse and pedestal levels, given our contrast and

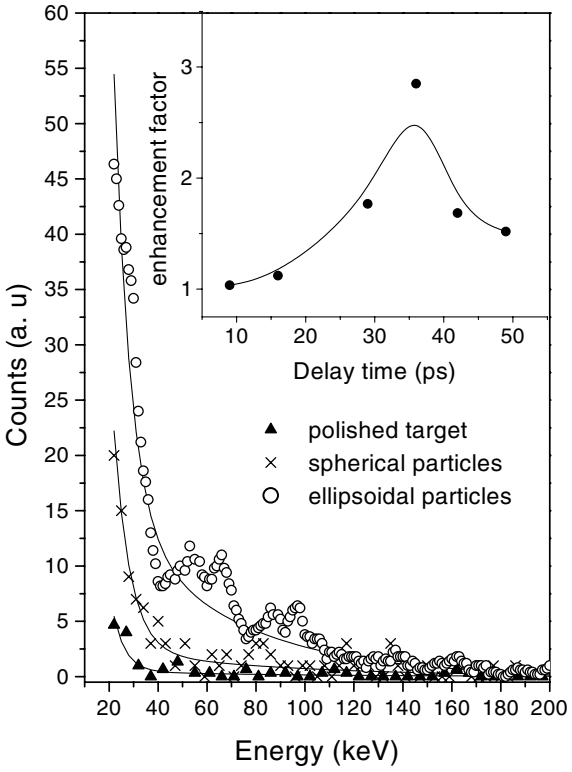

FIG. 4. Comparison of bremsstrahlung emission at 45°. Solid lines are temperature fits. Inset: Enhancement of emission with a preplasma formed at various delays. The solid line is a guide to the eye.

enhancement factors. Nevertheless, for the validity of our model, it is important to show that such a preplasma formation alone cannot explain the observed enhancement. Figure 4 (inset) provides the yield enhancements obtained from a polished target with an intentional preplasma formed before the main pulse incidence, at different delays. Intensities of the prepulse and main pulse were 5×10^{13} and 10^{15} W cm^{-2}, respectively. The maximum enhancement, even with this strong a prepulse, is only threefold, far below that yielded by the nanostructures. Thus, it is evident that the nanostructures are preserved until the main pulse. Further, it is expected that a preplasma formation would destroy the structure and adversely affect enhancement [9]. Thus, the observed enhancements themselves substantiate the integrity of the structure and the irrelevance of preformed plasma in our case.

In summary, we report a 13-fold enhancement of the total bremsstrahlung emission in the 10–200 keV range from a copper nanoparticle-coated target in comparison to an optically polished Cu target. A simple model of the surface shows that enhancements in local electromagnetic fields result in excess absorption and hotter electrons that, in turn, enhance x-ray emission. Such enhanced emission is very attractive for practically viable hard x-ray sources. Further, our model provides guidance for designing better sources of ultrashort hard x-ray pulses. The intensity levels we have used in this study are quite modest and are easily available from modern femtosecond lasers operating at multi-kHz repetition rates, making applications of nanoparticle-coated targets very promising.

The authors thank N. Kulkarni for help in experiments and S. Bhattacharya, N. Trivedi, M. Krishnamurthy, V. Kumarappan, and D. Mathur for useful discussions. The laser facility was partially funded by the Department of Science and Technology.

*Electronic address: grk@tifr.res.in

[1] Z. Jiang *et al.*, Phys. Plasmas **2**, 1702 (1995); P. Audebert *et al.*, Europhys. Lett. **19**, 189 (1992); U. Teubner *et al.*, Appl. Phys. B **62**, 213 (1996).
[2] C. W. Siders *et al.*, Science **286**, 1340 (1999); A. Cavalleri *et al.*, Phys. Rev. Lett. **87**, 237401 (2001).
[3] D. G. Stearns *et al.*, Phys. Rev. A **37**, 1684 (1988).
[4] T. Nishikawa *et al.*, Appl. Phys. Lett. **70**, 1653 (1997).
[5] M. M. Murnane *et al.*, Appl. Phys. Lett. **62**, 1068 (1993).
[6] C. Wulker *et al.*, Appl. Phys. Lett. **68**, 1338 (1996).
[7] J. C. Gauthier *et al.*, Proc. SPIE-Int. Soc. Opt. Eng. **2523**, 242 (1995).
[8] S. P. Gordon *et al.*, Opt. Lett. **19**, 484 (1994).
[9] G. Kulcsar *et al.*, Phys. Rev. Lett. **84**, 5149 (2000).
[10] T. Nishikawa *et al.*, Appl. Phys. B **73**, 185 (2001).
[11] W. L. Kruer, *The Physics of Laser-Plasma Interactions* (Addison-Wesley, Reading, MA, 1988).
[12] M. Tabak *et al.*, Phys. Plasmas **1**, 1626 (1994).
[13] S. C. Wilks *et al.*, Phys. Plasmas **8**, 542 (2001).
[14] V. M. Shalaev, *Nonlinear Optics of Random Media* (Springer-Verlag, Berlin, 2000).
[15] S. Banerjee *et al.*, Eur. Phys. J. D **11**, 295 (2000).
[16] G. F. Knoll, *Radiation Detection and Measurement* (Wiley, New York, 1989).
[17] P. Ayyub *et al.*, Appl. Phys. A **73**, 67 (2001).
[18] C. G. Granqvist and O. Hunderi, Phys. Rev. B **16**, 3513 (1977).
[19] L. Genzel, T. P. Martin, and U. Kreibig, Z. Phys. B **21**, 339 (1975).
[20] P. Taneja, P. Ayyub, and R. Chandra, Phys. Rev. B **65**, 245412 (2002).
[21] U. Kreibig and C. V. Fragstein, Z. Phys. **224**, 307 (1969).
[22] G. T. Boyd *et al.*, Phys. Rev. B **30**, 519 (1984).
[23] J. Gersten and A. Nitzan, J. Chem. Phys. **73**, 3023 (1980).
[24] T. Ditmire *et al.*, Phys. Rev. A **57**, 369 (1998).
[25] M. K. Grimes *et al.*, Phys. Rev. Lett. **82**, 4010 (1999).
[26] P. P. Rajeev *et al.*, Phys. Rev. A **65**, 052903 (2002).
[27] J. Kupersztych, P. Monchicourt, and M. Raynaud, Phys. Rev. Lett. **86**, 5180 (2001).
[28] Y. Zhang *et al.*, Opt. Commun. **126**, 85 (1996).